Lignin–Hydroxycinnamyl Model Compounds Related to Forage Cell Wall Structure. 1. Ether-Linked Structures

Richard F. Helm*,† and John Ralph†,‡

U.S. Dairy Forage Research Center, Agricultural Research Service, U.S. Department of Agriculture, 1925 Linden Drive West, Madison, Wisconsin 53706, and Department of Forestry, University of Wisconsin—Madison, Madison, Wisconsin 53706

A series of lignin–hydroxycinnamyl methyl ester model compounds have been synthesized and characterized by NMR spectroscopy. The materials represent several of the possible ether linkages analogous to the predominant β-*O*-4 structure of native lignins. The α-etherified model trimers were prepared by nucleophilic attack of the phenolate anion of methyl *p*-coumarate and methyl ferulate on the quinone methide of guaiacylglycerol–β-guaiacyl ether. Combined threo/erythro yields ranged from 40 to 67%, with methyl *p*-coumarate addition affording a significantly higher yield. The β-*O*-4-cinnamyl ether dimers were prepared according to established strategies for the β-*O*-4 lignin model dimers, with a modified hydroxymethylation step providing an alternative to the classical method. Zinc borohydride reduction of the α-keto-β-cinnamyl ethers proved to be quite useful for the enrichment of the *erythro*-β-ethers. Complete spectroscopic characterization of the models as well as their peracetates by one- and two-dimensional NMR spectroscopy provided important chemical shift data for the evolving lignin NMR database as well as for comparison with native tissue isolates and synthetic DHP lignins.

INTRODUCTION

The identification and characterization of a possible bridge between lignin and polysaccharides through hydroxycinnamic acids is an area of active research (Fry and Miller, 1989; Yamamoto et al., 1989). There is substantial information on the attachment of ferulic (4-hydroxy-3-methoxy-*trans*-cinnamic) and *p*-coumaric (4-hydroxy-*trans*-cinnamic) acids to arabinoxylans and xyloglucans (Ishii, 1991; Mueller-Harvey et al., 1986). However, there is considerably less information on the attachment of hydroxycinnamic acids to lignin (Scalbert et al., 1985, 1986) and still only indirect evidence for the cross-linking between lignin and polysaccharide through hydroxycinnamic acids (Iiyama, 1990; Kondo et al., 1990; Lam et al., 1990, 1992). Such bridges may directly influence cell wall development and degradation (Bacic et al., 1988; Lewis, 1990), and the quantification of this interaction is the first step toward understanding its role in plant cell wall development and degradation.

The reaction sites available to hydroxycinnamoyl esters during free-radical condensation reactions (i.e., lignification) have been described (Ralph and Helm, 1992; Ralph et al., 1992a). The incorporation is by classical free-radical mechanisms (active incorporation) and/or "opportunistic" passive incorporation via addition to intermediate quinone methides. As our investigations into the role of hydroxycinnamic acids in forage cell wall structure rely heavily on the use of NMR spectroscopy, appropriate models were needed to describe the theorized reaction sites. Synthetic strategies centered on structures related to the lignin guaiacylglycerol β-*O*-4-guaiacyl ether subunit, which is the predominant linkage found in native lignin. The results of our preparation and characterization of the α- and β-ethers are described here, and a forthcoming paper will address the synthetic and spectroscopic aspects of lignin–hydroxycinnamic acid ester models that are also related to the β-*O*-4 ether structure.

* Author to whom correspondence should be addressed.
† U.S. Dairy Forage Research Center.
‡ University of Wisconsin.

EXPERIMENTAL METHODS

General. Melting points are uncorrected. The standard reaction techniques, processing protocols, and chromatographic separation/purification schemes used throughout this investigation have already been outlined (Helm et al., 1991). Efforts were taken so that reactions involving materials containing a *trans*-cinnamyl moiety were performed in the dark, and final products were stored in a desiccator below 0 °C.

NMR Spectroscopy. NMR experiments were performed with a Bruker AMX-360 360-MHz instrument fitted with a 5-mm QNP probe (normal geometry) maintained at 300 K. The standard conditions used for all analyses were 15–25 mg of material in 450 μL of acetone-d_6, with the central solvent peak used as internal reference (δ_H 2.04, δ_C 29.8). The carbon and proton designations are based in standard lignin nomenclature (see figures). Two-dimensional correlation spectra were obtained with Bruker pulse programs, COSY spectra were double quantum filtered variants (cosydf or cosydftp), and phase-sensitive TOCSY spectra were obtained with the "mlevtp" microprogram; 2K data points in t_2, 256 increments, and 8 scans/increment were sufficient for all experiments. ^{13}C–^{1}H correlation experiments were performed by operating the QNP probe in the inverse mode. One-bond correlations were obtained using the standard phase-sensitive HMQC experiment (Bruker's invbtp) with 8–16 scans/128–256 increments, each acquiring 2K data points. Long-range HMBC correlations were obtained with 16–96 scans/256 increments. Standard apodization and processing procedures were used (Ralph et al., 1992a). Samples for which multiplicity problems with OH–OD exchange were encountered were exchanged with D_2O prior to analysis.

Methyl 4-Hydroxycinnamates. *p*-Coumaric acid (9.08 g, 55 mmol) was dissolved in methanolic BF_3 (~12 wt %, 125 mL) and heated to 60 °C for 2 h (Allen, 1972). The resulting mixture was cooled to room temperature and added to a well-stirred solution of ice–water. The precipitate which formed was isolated by filtration and washed with H_2O. The solid was dissolved in Et_2O and processed. Crystallization from acetone–light petroleum ether (bp 40–60 °C) gave **2** in two crops (8.36 g, 85%): mp 139.5–141 °C; ^{13}C NMR δ (acetone-d_6) 51.47 (OMe), 115.30 (C-8), 116.66 (C-3,5), 126.97 (C-1), 130.89 (C-2,6), 145.34 (C-7), 160.53 (C-4), 167.84 (C-9).

Methyl ferulate (**3**) was prepared in the same fashion with the crude reaction product being poured into an ice-cold solution of saturated aqueous $NaHCO_3$, and the mixture was extracted with Et_2O (2×). The organic layer was washed successively with

aqueous NaCl and NH_4Cl (2×) and processed. Crystallization (three crops) from Et_2O gave **3** in 83% yield: mp 67–68 °C; ^{13}C NMR δ (acetone-d_6) 51.47 (OMe), 56.32 (Ar OMe), 111.35 (F-2), 115.53 (F-8), 116.06 (F-5), 123.85 (F-6), 127.40 (F-1), 145.69 (F-7), 148.73 (F-3), 150.06 (F-4), 167.85 (F-9).

Methyl sinapate (**4**) was prepared by dissolving 3,5-dimethoxy-4-hydroxy-*trans*-cinnamic acid (5.03 g, 22.4 mmol) in methanolic HCl, freshly prepared by the addition of acetyl chloride (2.5 mL) to MeOH (50 mL). The solution was heated until all starting material had dissolved and was left to cool without stirring. Crystallization began slowly with additional material forming upon storage below 0 °C. Isolation of the solid by filtration and washing with H_2O gave **4** (4.51 g, 84%) as white needles: mp 93.5–94 °C; ^{13}C NMR δ (acetone-d_6) 51.48 (OMe), 56.67 (Ar OMe), 106.84 (S-2,6), 115.76 (S-8), 126.11 (S-1), 139.46 (S-4), 146.03 (S-7), 148.92 (S-3,5), 167.84 (S-9).

α-Etherification. A threo/erythro mixture of 1-(4-hydroxy-3-methoxyphenyl)-2-(2-methoxyphenoxy)propane-1,3-diol (**1**) (Nakatsubo, 1975; Ralph and Young, 1981) was converted to the quinone methide (**1a**) according to the method of Ralph and Young (1983). Compound **1** (970 mg, 3.03 mmol) was dissolved in CH_2Cl_2 (100 mL) in a 250-mL separatory funnel. To this solution was added trimethylsilyl bromide (0.80 mL, 6.1 mmol), and the solution was shaken slightly. The mixture was left for 15 min, after which time cold, aqueous, saturated $NaHCO_3$ was added. The funnel was shaken, and the yellow organic layer, which contained **1a**, was dried (Na_2SO_4) and filtered (total volume approximately 150 mL).

Methyl *p*-coumarate (**2**, 1.082 g, 6.07 mmol) was suspended in CH_2Cl_2 (50 mL) and 1,8-diazabicyclo[5.4.0]-undec-7-ene (DBU, 30 μL, 0.07 mmol) was added via a syringe with stirring. This solution was added dropwise to the stirred solution of **1a**, and the resulting mixture was left without stirring overnight. Evaporation to a syrup and purification by silica gel chromatography ($CHCl_3$–EtOAc, 9:1) afforded methyl 4-[3-hydroxy-1-(4-hydroxy-3-methoxyphenyl)-2-(2-methoxyphenyl)propyl]-*p*-coumarate (**5**-*erythro*, 750 mg; **5**-*threo*, 200 mg) in 67% combined yield.

Compound **6** was prepared as described for **5** with the use of **3** in the addition step. Separation of the threo/erythro isomers by silica gel chromatography provided methyl 4-[3-hydroxy-1-(4-hydroxy-3-methoxyphenyl)-2-(2-methoxyphenoxy)propyl]ferulate (**6**-*threo* and **6**-*erythro*, 39% combined yield) in approximately a 1:1 ratio.

4-Acetoxy-α-bromo-3-methoxyacetophenone (8). Acetovanillone (**7**, 25.02 g, 151 mmol) was dissolved in pyridine (50 mL) and acetic anhydride (45 mL) and left overnight. The reaction was quenched with absolute EtOH, and the reaction volume was reduced in volume to ~50 mL by evaporation under reduced pressure (50 °C). The thick solution was diluted with CH_2Cl_2 and washed with H_2O (3×). Processing and crystallization from EtOH–H_2O gave 4-acetoxy-3-methoxyacetophenone (27.6 g, 88%, mp 59–60 °C). A portion of the acetate (5.03 g, 24.2 mmol) was dissolved in CCl_4–$CHCl_3$ (175 mL, 6:1) in a 250-mL separatory funnel and Br_2 (4.09 g, 25.6 mmol) was added (Landucci et al., 1981). Nitrogen gas was bubbled continuously through the solution for 40 min, when the mixture was washed with cold aqueous $NaHCO_3$ and processed. Crystallization (two crops) from MeOH gave **8** as small needles (6.23 g, 90%): mp 88.5–89 °C; ^{13}C NMR δ (acetone-d_6) 20.44 (Ac), 32.91 (β), 56.50 (Ar OMe), 113.18 (A-2), 122.99 (A-6), 124.06 (A-5), 133.85 (A-1), 145.40 (A-4), 152.65 (A-3), 168.59 (Ac), 191.01 (α).

Methyl 4-Hydroxycinnamate Addition. Compound **8** (2.00 g, 6.97 mmol) was added to a solution of **2** (1.30 g, 7.31 mmol) and powdered K_2CO_3 (1.00 g) in acetone (75 mL). The reaction was refluxed until complete disappearance of **8** was noted by TLC ($CHCl_3$–EtOAc, 1:1) (5 h), the solution was filtered, and the filtrate was evaporated to a solid. Crystallization from acetone afforded **9** as small needles (1.80 g, 67%): mp 167.5–169 °C; ^{13}C NMR δ (DMSO-d_6) 20.37 (Ac), 51.29 (OMe), 56.09 (Ar OMe), 70.15 (β), 111.66 (A-2), 115.09 (C-3,5), 115.32 (C-8), 121.2 (A-6), 123.34 (A-5), 127.00 (C-1), 130.03 (C-2,6), 133.04 (A-1), 143.74 (A-4), 144.22 (C-7), 151.18 (A-3), 159.84 (C-4), 166.91 (C-9), 168.18 (Ac), 193.21 (α).

Compound **10** was prepared in the same fashion with **3** as the nucleophile (2.5-h reaction time). Processing and crystallization (absolute EtOH) gave **10** as white needles (94%): mp 131–134 °C; ^{13}C NMR δ (DMSO-d_6) 20.35 (Ac), 51.28 (OMe), 55.75 and 56.06 (Ar OMe), 70.56 (β), 111.09 (F-2), 111.71 (A-2), 113.14 (F-5), 115.57 (F-8), 121.20 (A-6), 122.48 (F-6), 123.32 (A-5), 127.40 (F-1), 133.07 (A-1), 143.73 (A-4), 144.59 (F-7), 149.05 (F-4), 149.55 (F-3), 151.17 (A-3), 166.96 (F-9), 168.19 (Ac), 193.26 (α).

Compound **11** was prepared in the same fashion with **4** as the nucleophile (7-h reaction time). Processing and crystallization (absolute EtOH) gave **11** as white needles (91%): mp 136–136.5 °C; ^{13}C NMR δ (DMSO-d_6) 20.36 (Ac), 51.38 (OMe), 56.00 and 56.11 (Ar OMe), 74.47 (β), 106.04 (S-2,6), 111.82 (A-2), 117.18 (S-8), 121.28 (A-6), 123.21 (A-5), 129.68 (S-1), 133.38 (A-1), 137.83 (S-4), 143.45 (A-4), 144.65 (S-7), 151.06 (A-3), 152.50 (S-3,5), 166.80 (S-9), 168.18 (Ac), 193.68 (α).

Hydroxymethylation. Compound **9**, **10**, or **11** (1.02 mmol) was dissolved in dioxane (15 mL), and powdered K_2CO_3 (1.06 g, 7.7 mmol) was added, followed by aqueous H_2CO (37 wt %, 150 μL, 2.0 mmol). The reaction was stirred vigorously, with the conversion being monitored by TLC ($CHCl_3$–EtOAc, 1:1). After almost complete disappearance of the starting material (3.5–24 h), the mixture was filtered and the filtrate was evaporated to a syrup. The syrup was dissolved in EtOAc and washed with aqueous NH_4Cl (2×). Processing and silica gel chromatography gave the desired β-hydroxymethylated addition products (**9a**–**11a**).

Compound **9a** was purified by silica gel chromatography (40 g of silica, $CHCl_3$–EtOAc, 8:1). Crystallization from acetone–light petroleum ether afforded small needles in 61% yield: mp 151–152 °C; ^{13}C NMR δ (acetone-d_6) 20.44 (Ac), 51.54 (OMe), 56.43 (Ar OMe), 63.90 (γ), 82.32 (β), 113.13 (A-2), 116.42 (C-3,5), 116.49 (C-8), 122.75 (A-6), 124.06 (A-5), 128.57 (C-1), 130.69 (C-2,6), 134.83 (A-1), 144.78 (C-7), 145.39 (A-4), 152.60 (A-3), 160.59 (C-4), 167.65 (C-9), 168.60 (Ac), 195.78 (α).

Compound **10a** was purified by silica gel chromatography (40 g of silica, $CHCl_3$–EtOAc, 4.5:1) as a clear syrup in 77% yield: ^{13}C NMR δ (acetone-d_6) 20.44 (Ac), 51.55 (OMe), 56.30 and 56.38 (Ar OMe), 63.90 (γ), 83.78 (β), 112.28 (F-2), 113.37 (A-2), 116.24 (F-5), 116.88 (F-8), 122.79 (A-6), 123.04 (F-6), 123.90 (A-5), 129.54 (F-1), 135.02 (A-1), 145.08 (F-7), 145.19 (A-4), 150.28 (F-4), 151.02 (F-3), 152.43 (A-3), 167.65 (F-9), 168.60 (Ac), 196.19 (α).

Compound **11a** was purified by silica gel chromatography (40 g of silica, $CHCl_3$–EtOAc, 9:1). Crystallization from acetone–light petroleum ether afforded small needles in 70% yield: mp 133–134.5 °C; ^{13}C NMR δ (acetone-d_6) 20.46 (Ac), 51.65 (OMe), 56.41 and 56.51 (Ar OMe), 63.67 (γ), 86.84 (β), 106.49 (S-2,6), 113.39 (A-2), 118.22 (S-8), 122.87 (A-6), 123.68 (A-5), 131.25 (S-1), 135.73 (A-1), 139.07 (S-4), 144.81 (A-4), 145.24 (S-7), 152.33 (A-3), 153.71 (S-3,5), 167.53 (S-9), 168.65 (Ac), 196.07 (α).

Borohydride Reductions. *A. $NaBH_4$.* The α-keto-β-cinnamyl compounds (**9a**–**11a**) were treated overnight with excess $NaBH_4$ in MeOH–H_2O. For example, the starting material (1 mmol) was dissolved in MeOH (8.5 mL), and H_2O (6 mL) followed by sodium borohydride (300 mg) was added; the mixture was left overnight. The reaction was quenched with HOAc and evaporated to an aqueous–solid matrix. Dissolution of the solid in EtOAc, washing with aqueous NH_4Cl (3×), and processing gave the crude products in over 90% yield.

Methyl 4-[2-hydroxy-2-(4-hydroxy-3-methoxyphenyl)-1-(hydroxymethyl)ethyl]-*p*-coumarate (**12**) was obtained from silica gel chromatography ($CHCl_3$–EtOAc, 1:1) as a 70:30 (threo/erythro) mixture.

Methyl 4-[2-hydroxy-2-(4-hydroxy-3-methoxyphenyl)-1-(hydroxymethyl)ethyl]ferulate (**13**) was purified by silica gel chromatography ($CHCl_3$–EtOAc, 1:1) as a 70:30 (threo/erythro) mixture.

Methyl 4-[2-hydroxy-2-(4-hydroxy-3-methoxyphenyl)-1-(hydroxymethyl)ethyl]sinapate (**14**) was purified by silica gel chromatography ($CHCl_3$–EtOAc, 1:1) as a 95:5 (threo/erythro) mixture.

B. $Zn(BH_4)_2$. Zinc borohydride (~0.16 M) in dry Et_2O was prepared according to the method of Gensler et al. (1960). The α-keto-β-ferulyl (**10a**) and -sinapyl (**11a**) compounds (120 mg) were dissolved in dry benzene (5 mL) and cooled to ca. 10 °C. The ethereal $Zn(BH_4)_2$ (5 mL) was added, and TLC indicated that the reaction was complete within 1 h. The excess borohydride was quenched by the slow addition of H_2O followed by HOAc. The α-keto-β-(*p*-coumaryl) compound (**9a**) was reduced in the

same manner using dry EtOAc instead of benzene. The quenched reaction mixture was diluted with EtOAc, washed with aqueous NH_4Cl (2×), and processed. Purification by silica gel chromatography gave compounds **12a**, **13a**, and **14a**.

Methyl 4-[2-(4-acetoxy-3-methoxyphenyl)-2-hydroxy-1-(hydroxymethyl)ethyl]-*p*-coumarate (**12a**) was isolated by silica gel chromatography ($CHCl_3$–EtOAc, 1:1) as a threo/erythro mixture (55:45) in 81% yield: ^{13}C NMR δ (acetone-d_6) threo 61.70 (γ), 73.21 (α), 83.90 (β); erythro 61.87 (γ), 73.57 (α), 83.65 (β).

Methyl 4-[2-(4-acetoxy-3-methoxyphenyl)-2-hydroxy-1-(hydroxymethyl)ethyl]ferulate (**13a**) was isolated by silica gel chromatography ($CHCl_3$–EtOAc, 1:1) as a threo/erythro mixture (52:48) in 87% yield: ^{13}C NMR δ (acetone-d_6) threo 61.84 (γ), 73.38 (α), 85.57 (β); erythro 61.84 (γ), 73.62 (α), 85.47 (β).

Methyl 4-[2-(4-acetoxy-3-methoxyphenyl)-2-hydroxy-1-(hydroxymethyl)ethyl]sinapate (**14a**) was isolated by silica gel chromatography ($CHCl_3$–EtOAc, 3:1) with the threo and erythro isomers (70:30) separable in 91% combined yield: ^{13}C NMR δ (acetone-d_6) threo 61.62 (γ), 73.67 (α), 88.99 (β); erythro 60.89 (γ), 73.28 (α), 87.66 (β).

Deacetylation was accomplished by treatment with $NaHCO_3$ in MeOH–H_2O (Greene and Wuts, 1991). The 4-acetate (0.11 mmol) was dissolved in MeOH (2 mL), and H_2O (1 mL) was added followed by saturated aqueous $NaHCO_3$ (1 mL). The reaction was stirred slowly for 2 h and quenched with 3% HCl. The aqueous solution was mixed with EtOAc and washed (2×). The combined organic phase was washed with aqueous NH_4Cl (2×) and processed to afford compounds **12**–**14** in almost quantitative yield.

RESULTS AND DISCUSSION

Synthetic Aspects. The α-etherification reaction of the phenolate anion of **3** and **1a** has been reported previously (Scalbert et al., 1986) with the coupling conditions affording only one characterized racemic isomer (which was not assigned a stereochemistry). As both isomers (racemic) were desired, studies were undertaken to identify methods by which both isomers could be prepared using **2** and **3** as nucleophiles. Repeating the method of Scalbert et al. (1986) did indeed provide an initial production of major (erythro) and minor (threo) isomeric α-ethers (further discussion of stereochemistry and proton assignments will be reserved for later). Although the final thermodynamic equilibrium was not rigorously examined, **6** readily achieved a 50:50 threo:erythro ratio after 12 h, whereas **5** produced a 20:80 threo:erythro ratio. Increasing the reaction time increased the relative proportion of the minor (threo) component, but the overall yield remained the same (±2%).

Thus, having established the "equilibrium" nature of the system, we began testing other base-catalyzed reaction systems in efforts to improve the reaction yield. Only a moderate yield increase was achieved, but the use of DBU as the base catalyst was found to be more convenient. The higher yield of the *p*-coumaryl ethers (67%) compared to the feruloyl ethers (40%) is noteworthy. This is probably a manifestation of the higher nucleophilicity of **2** relative to that of **3** (Leary et al., 1977), as well as the reduced sterics associated with approaching **1a** by a nucleophile lacking a 3-methoxy substituent (Nakatsubo et al., 1976). Only moderate increases in the yield of the thermodynamic isomer of **5** (threo) were achieved with longer reaction times. This suggests that the *p*-coumaryl α-ethers are less susceptible to α-cleavage relative to the feruloyl isomers (**6**). A result of the facile nature of α-cleavage of the kinetically favored **6**-*erythro* is that decomposition occurs during storage at room temperature, especially when in contact with aqueous solvents. The **5** isomers as well as the thermodynamically favored **6**-*threo* are much less susceptible to decomposition.

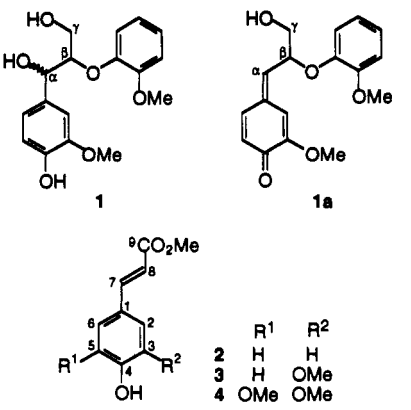

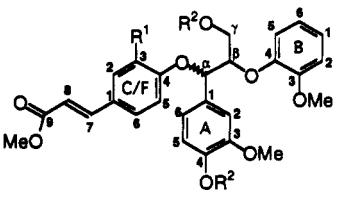

The synthetic strategy for the production of the β-cinnamyl ethers is outlined in Scheme I and follows the

Scheme I. Synthesis of Guaiacylglycerol-β-Hydroxycinnamyl Ethers[a]

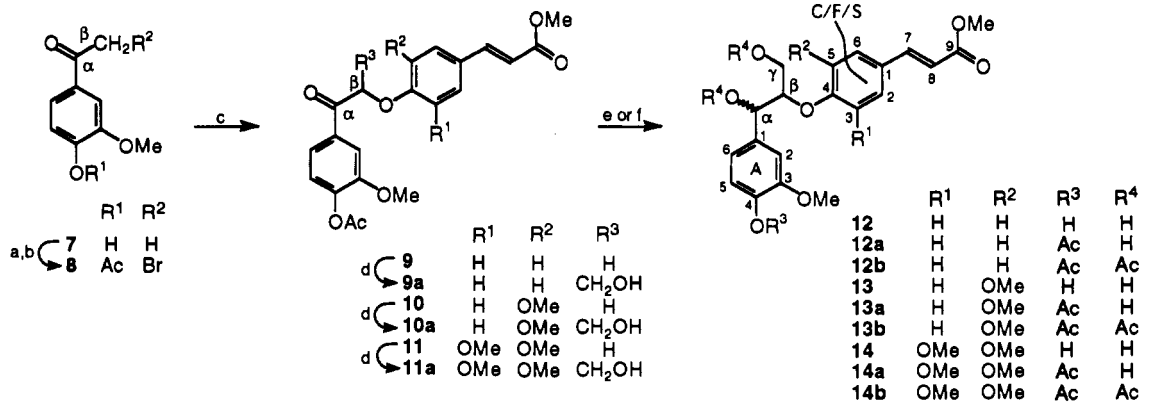

[a] a, Ac_2O/pyridine; b, Br_2–$CHCl_3/CCl_4$; c, methyl *p*-coumarate/ferulate/sinapate, K_2CO_3; d, H_2CO, K_2CO_3; e, $NaBH_4$–MeOH/H_2O; f, $Zn(BH_4)_2$ then $NaHCO_3$–MeOH/H_2O.

Table I. Selected ^{1}H NMR Data for the Model Dimers and Trimers and Their Corresponding Peracetates[a]

compd	C/F/S-7 ($J_{7,8}$)	C/F/S-8	α ($J_{\alpha,\beta}$)	β	γ ($J_{\gamma,\beta}$)	γ' ($J_{\gamma',\beta}$)
5-*threo*	7.55 (16.0)	6.33	5.60 (6.4)	4.54	3.53 (5.4)	3.72 (4.1)
5-*erythro*	7.56 (16.0)	6.34	5.60 (5.4)	4.59	3.80 (4.2)	3.92 (5.3)
5a-*threo*	7.56 (16.0)	6.35	5.74 (5.7)	4.87	4.12 (5.7)	4.34 (4.3)
5a-*erythro*	7.57 (16.0)	6.36	5.75 (5.4)	4.84	4.41 (4.2)	4.52 (5.3)
6-*threo*	7.53 (15.9)	6.36	5.61 (6.3)	4.53	3.53 (5.9)	3.70 (4.0)
6-*erythro*	7.53 (15.9)	6.38	5.56 (5.5)	4.56	3.83 (4.5)	3.93 (5.1)
6a-*threo*	7.54 (16.0)	6.39	5.75 (5.4)	4.87	4.15 (3.9)	4.37 (5.9)
6a-*erythro*	7.55 (16.0)	6.40	5.72 (5.2)	4.85	4.45 (5.8)	4.55 (3.9)
12-*threo*	7.59 (16.0)	6.36	4.93 (5.3)	4.56	3.57 (5.7)	3.80 (4.0)
12-*erythro*	7.57 (16.0)	6.35	4.90 (5.8)	4.56	3.86[b] (4.5)	3.86[b] (4.5)
12b-*threo*	7.61 (16.1)	6.41	6.11 (6.5)	5.06	4.10 (6.0)	4.27 (3.9)
12b-*erythro*	7.62 (16.1)	6.40	6.06 (5.5)	5.06	4.31 (4.1)	4.37 (5.9)
13-*threo*	7.59 (16.0)	6.43	4.89 (7.0)	4.38	3.54 (5.9)	3.72 (3.5)
13-*erythro*	7.57 (16.0)	6.41	4.90 (6.5)	4.46	3.76 (4.1)	3.83 (5.5)
13b-*threo*	7.60 (16.0)	6.46	6.11 (6.5)	4.97	4.06 (5.8)	4.28 (4.1)
13b-*erythro*	7.59 (16.0)	6.45	6.07 (5.2)	4.93	4.25 (4.1)	4.37 (6.0)
14-*threo*	7.60 (16.0)	6.53	5.00 (7.2)	4.04	3.31 (3.4)	3.68 (3.6)
14-*erythro*	7.61 (16.0)	6.53	4.99 (4.5)	4.26	3.47 (3.5)	3.86 (5.9)
14b-*threo*	7.60 (16.0)	6.52	6.13 (6.9)	4.71	3.92 (4.7)	4.28 (4.0)
14b-*erythro*	7.61 (16.0)	6.53	6.10 (4.5)	4.82	4.19 (4.0)	4.43 (6.1)

[a] In ppm. Coupling constants are listed in parentheses and are measured to within ±0.05 Hz. Proton designations are based on standard lignin nomenclature (see figures). Recorded in acetone-d_6 at 300 K on materials that had been freeze-dried from D_2O. [b] Equivalent protons (i.e., no $J_{\gamma,\gamma'}$).

standard route to the β-*O*-4 ethers. The 4-hydroxy position of acetovanillone was protected by acetylation. The use of a benzyl protecting group is not compatible the α,β-double bond of cinnamyl groups since cleavage by hydrogenation also reduces the α,β-double bond. Formation of bromide (**8**) and coupling with **2**, **3**, and **4** afforded the crystalline β-cinnamyl ethers (**9**, **10**, and **11**, respectively) in good yields. The hydroxymethylation step proved to be the most difficult transformation in the synthetic scheme. Classical methods (Landucci et al., 1981) afforded only low yields (25%) of the desired materials with A-ring deacetylation and β-hydroxymethylation/dehydration as well as di-β-methylolation occurring. After numerous reaction modifications and approaches were attempted, the best method with respect to simplicity and yield was found to be the use of aqueous formaldehyde in dioxane at room temperature with an excess of powdered K_2CO_3. These reaction conditions afforded the pure formaldehyde addition products (**9a**–**11a**) in 61–77% yield.

Reduction of the α-keto group and deacetylation provided the desired β-cinnamyl ethers. Sodium borohydride ($NaBH_4$) reduction in MeOH–H_2O gave the predominantly threo products (Ralph and Helm, 1991) with concomitant deacetylation. The use of EtOH–H_2O, the standard solvent system employed for preferential threo production of lignin models (Barelle et al., 1989; Brunow et al., 1988), also provided the threo/erythro isomers in a 70:30 ratio but effected transesterification of the methyl ester as well. Since $NaBH_4$ gave predominantly the threo isomers of **12**–**14**, additional methodology was required to prepare higher proportions of the erythro isomers. There have been reports in the literature (Brunow et al., 1988; Nakata and Oishi, 1980) that zinc borohydride [$Zn(BH_4)_2$] favored formation of the erythro isomers of somewhat similar model compounds. Indeed, the reduction of **9a**, **10a**, and **11a** in Et_2O gave significantly higher proportions of the erythro isomers (**12a**, **13a**, and **14a**, respectively). The aprotic conditions did not afford cleavage of the 4-acetate, and subsequent removal was accomplished by treatment with $NaHCO_3$ in MeOH–H_2O. Compounds **12** and **13** were prepared in an approximately 1:1 threo:erythro ratio, while **14** was prepared in a 65:35 (threo:erythro) ratio. The threo:erythro isomers of **14a** were separable by silica gel chromatography. Therefore, purification and subsequent deacetylation gave purified **14**-*threo* and **14**-*erythro* racemates for subsequent spectroscopic characterization.

The synthetic scheme described for the β-cinnamyl ethers represents the first major effort to prepare proposed enzyme-induced lignin–hydroxycinnamic acid condensation products related to the β-*O*-4 linkage. The β-feruloyl ether (**13**) had been prepared by Katayama et al. (1981) by a slightly more arduous synthetic pathway. The advantages of the procedure described in this work include the flexibility of the β-addition reaction to **8**, the facile conditions for most steps subsequent to that transformation, and the typically high-yielding reactions. Further synthetic work utilizing this basic strategy involves the preparation of lignin–hydroxycinnamic acid–polysaccharide model compounds (Ralph et al., 1992b).

Spectroscopic Aspects. *A. Proton Assignments.* The first step in spectral characterization of β-*O*-4 models is the designation of threo and erythro stereochemistry. The chemical shifts and coupling constants for the side-chain protons of samples that had been freeze-dried from D_2O are shown in Table I (exchanging the hydroxyl protons with deuterons eliminates their coupling with vicinal protons). Whereas the isomeric distribution for compounds **5** and **6** arises from the addition of the phenolate anions of **2** and **3** to the quinone methide of **1**, the isomers of **12**–**14** result from the borohydride reduction of the α-carbonyl (Scheme I). The isomers of **12**–**14** can be readily assigned, as mentioned previously, due to the choice of reductant and reduction solvent system. Additional evidence for stereochemical assignments is provided by the chemical shifts of the α-hydroxyl protons in acetone-d_6. The chemical shifts of erythro α-hydroxyls in β-*O*-4 lignin models that we have thus far investigated are at a higher field relative to those of their threo counterparts (Ralph and Helm, 1991), and this was observed for **12**–**14**. The threo γ-protons typically have lower chemical shifts relative to their erythro companion isomers, and this trend has also been used in previous studies as the basis of assigning threo/erythro stereochemistry (Katayama et al., 1987; Brunow et al., 1989). This general rule applied to all of the compounds investigated in this work with the exception of the β-sinapyl models **14** and **14b**. Although the most upfield γ-proton was still of the threo isomer, its geminal partner displayed a chemical shift intermediate to those of the γ-erythro multiplets.

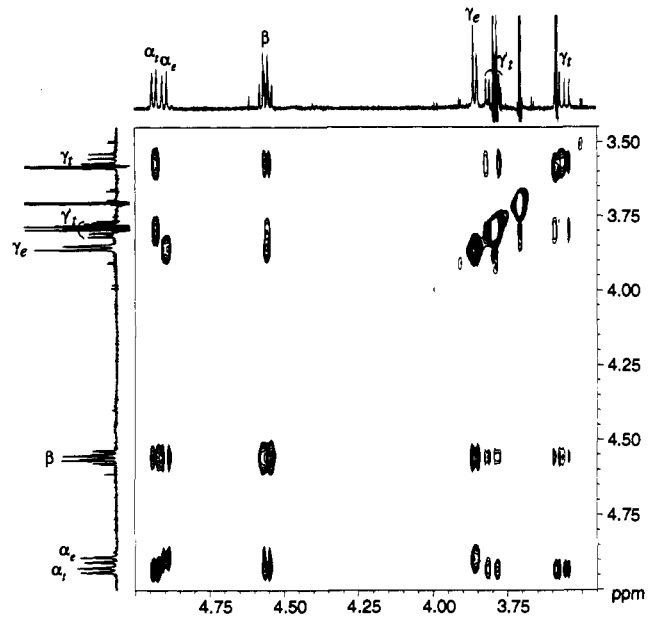

Figure 1. Portion of the phase-sensitive TOCSY spectrum of **12** (50:50 *threo*:*erythro* mixture) showing the region of the α-, β-, and γ-protons.

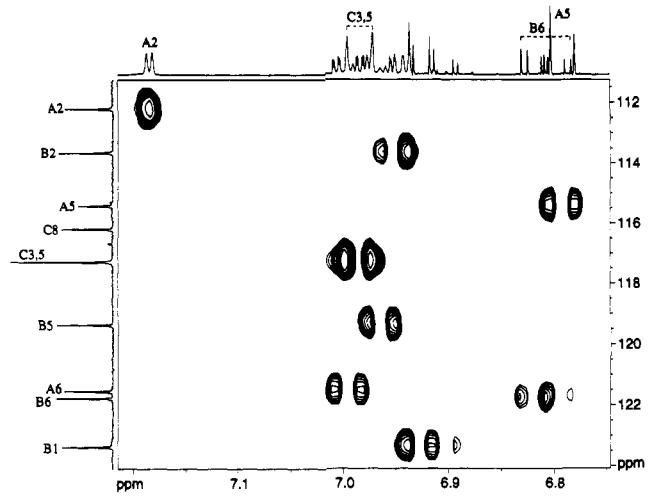

Figure 2. Congested aromatic region of **5**-*erythro* as correlated by the one-bond HMQC experiment.

It can be difficult to establish the chemical shifts of the γ-protons of the unacetylated model compounds due to interference by the methoxyl protons, and this often necessitates characterization of the peracetylated derivative to gain information on the "native" model. A great deal of information concerning the side-chain protons can be garnered from analysis of the TOCSY spectra of the unacetylated models. TOCSY, or total correlation spectroscopy, produces 2D ^1H–^1H spectra in which protons within the same coupling network are correlated with one another (Bax and Davis, 1985). Thus, with respect to the lignin models, all of the side-chain protons of the same isomer are correlated with one another. Due to the nature of the TOCSY experiment, phase cycling is not that critical, and the transfer of magnetization from one proton to another can occur starting from any position in the coupling network. Thus, as few as one scan per increment can be performed with a relatively short (0.5–1.0 s) relaxation delay. In other words, this 2D experiment can be run in about 7 min without any difficulty. We typically find that four scans per increment provide much more reliable correlations, and with 256 increments the experiment can be performed in 30 min.

Figure 1 displays the phase-sensitive TOCSY spectrum of **12**. This threo/erythro mixture was obtained via the $Zn(BH_4)_2$ reduction pathway, and the sample was freeze-dried from D_2O prior to analysis. The threo and erythro coupling networks are clearly displayed. The erythro γ-protons are equivalent and therefore degenerate into a doublet. The chemical shifts of the γ-protons can be obtained by selecting a row of the resultant 2D spectra, inverse Fourier transforming, zero-filling, and reprocessing. Although the resolution of coupling constants is only 1 Hz in this particular experiment, chemical shifts are readily obtained. Accurate determinations of the $J_{\beta,\gamma}$ coupling constants of obscured γ-protons can be accomplished by performing a higher resolution TOCSY experiment and reprocessing a selected row in the aforementioned way.

Some observations on the data presented in Table I are worth noting. There can be significant differences between the coupling constants of the free and acetylated models. As a typical example, the $J_{\alpha,\beta}$ of **5**-*threo* is 6.4 Hz, whereas for **5a**-*threo* it is 5.7 Hz. Generally, the coupling constant of the acetate is smaller than that of the free model. The $J_{\alpha,\beta}$ values for the threo isomers, both free and peracetylated, are greater than those of their erythro isomers in all cases with the exception of **12**. Relying on coupling constants for general stereochemical assignments is unreliable.

The assignment of stereochemistry to the quinone methide addition products (**5** and **6**) is based on the chemical shifts of the γ-protons. Thus, the kinetic product for addition to the quinone methide is the erythro isomer, with extended reaction times affording increasing amounts of the threo material. Organic acids have also been shown to provide the erythro product (Nakatsubo et al., 1976), whereas amines afforded the threo isomer almost exclusively (Ralph and Young, 1983). Katayama et al. (1987) and Brunow et al. (1989) obtained preferential erythro addition of the phenolate anion of vanillyl alcohol to quinone methides under neutral conditions. The addition of methyl ferulate to **1a** under basic conditions (Scalbert et al., 1986) provided only one isomer (which was not assigned a stereochemistry). As mentioned earlier, the lack of the other isomer resulted from the use of a short reaction time. We have found that the initial product under the conditions of Scalbert et al. (1986) was **6**-*erythro*.

The stereochemistry of the quinone methide of **1a** has been rigorously determined (Ralph et al., 1991) and was found to be two noninterconverting isomers differing in 3-methoxyl orientation. Only minor reactivity and steric differences between the two isomers have been noted (Ede et al., 1990). Thus, the spatial arrangement of the β- and γ-substituents must play an important role in the favored formation of the kinetic erythro product. Considering the facile nature of the decomposition of **6**-*erythro* as well as its rapid initial rate of formation, the combined bulk and electron-donating ability of the 3-methoxyl substituent may be a factor favoring cleavage of the ferulyl moiety. If this is true, then the α-sinapyl analog of **6** should be even more unstable. The differences in isomer stability (i.e., **6**-*threo* vs **6**-*erythro*) cannot be explained at this time. The instability of α-ethers suggests that the existence of free phenolic α-ethers may be somewhat limited in native lignin. Stability would only be induced if the free phenolic hydroxyl (A-ring) of the formed α-ether underwent a free-radical condensation reaction. Ede and Brunow (1992) have used TOCSY and HMQC techniques to investigate the structure of suspension culture lignin of Norway spruce and could not find any evidence of α-etherified structures, although other studies indicate isolable amounts can be produced (Freudenberg and Friedmann, 1960).

Table II. ^{13}C NMR Data for the Lignin–Hydroxycinnamyl Ether-Linked Model Trimers and Their Corresponding Peracetates[a,b]

	5		5a		6		6a	
carbon	*threo*	*erythro*	*threo*	*erythro*	*threo*	*erythro*	*threo*	*erythro*
α	80.96	79.56	80.55	79.65	81.37	80.90	81.08	80.69
β	86.19	85.22	81.71	81.72	86.57	85.46	81.63	81.85
γ	61.64	61.19	63.69	63.18	61.86	61.62	63.83	63.42
A-1	129.93	129.80	136.84	137.05	129.84	130.06	136.91	137.32
A-2	111.69	112.22	112.60	112.62	111.72	112.13	112.65	112.64
A-3	148.47	148.24	152.39	152.27	148.39	148.20	152.23	152.17
A-4	147.49	147.31	140.88	140.73	147.46	147.33	140.79	140.69
A-5	115.72	115.42	123.69	123.53	115.63	115.37	123.49	123.36
A-6	121.11	121.54	120.29	120.28	121.09	121.47	120.26	120.38
B-1	123.24	123.36	123.69	124.01	123.33	123.36	123.63	123.87
B-2	113.58	113.64	113.65	113.77	113.53	113.59	113.67	113.72
B-3	151.83	151.90	151.86	152.05	151.82	151.89	151.86	152.00
B-4	149.85	149.10	149.23	148.42	149.90	149.14	149.20	148.55
B-5	119.45	119.36	119.31	119.92	119.96	119.62	119.32	119.86
B-6	121.74	121.76	121.61	121.63	121.95	121.80	121.67	121.63
C/F-1	127.99	128.14	128.47	128.60	128.55	128.82	129.32	129.39
C/F-2	130.44	130.48	130.56	130.59	111.97	111.91	112.14	112.14
C/F-3	117.21	117.28	117.13	117.19	151.26	151.29	151.44	151.44
C/F-4	161.19	160.79	160.62	160.46	150.87	150.47	150.32	150.23
C/F-5	117.21	117.28	117.13	117.19	116.12	116.40	116.75	116.80
C/F-6	130.44	130.48	130.56	130.59	123.07	123.05	122.96	122.97
C/F-7	145.01	144.96	144.84	144.80	145.33	145.29	145.17	145.17
C/F-8	116.07	116.19	116.42	116.52	116.31	116.49	116.75	116.80
C/F-9	167.71	167.69	167.65	167.64	167.72	167.70	167.65	167.65

[a] Values were determined in acetone-d_6 at 300 K with the central solvent peak as internal reference (29.8 ppm). Carbon designations are based on standard lignin nomenclature (see figures). [b] Chemical shift assignments are based on one- and two-dimensional NMR experiments, and stereochemical designations are based on proton chemical shifts of the γ-protons.

Table III. ^{13}C NMR Data for the Lignin–Hydroxycinnamyl Ether-Linked Model Dimers[a]

	12		13		14	
carbon	*threo*	*erythro*	*threo*	*erythro*	*threo*	*erythro*
α	73.48	73.79	73.70	73.82	73.91	73.47
β	84.28	83.76	87.21	85.68	89.77	88.05
γ	61.85	62.06	61.94	61.98	61.49	61.02
A-1	134.06	134.19	133.73	134.08	133.58	133.71
A-2	111.36	111.41	111.39	111.53	111.41	110.93
A-3	148.02	147.94	148.02	147.91	147.92	147.97
A-4	146.79	146.71	146.84	146.68	146.79	146.50
A-5	115.26	115.18	115.21	115.08	115.21	115.21
A-6	120.38	120.53	120.47	120.57	120.66	120.07
C/F/S-1	127.85	127.86	129.23	129.09	131.23	131.16
C/F/S-2	130.50	130.45	112.01	112.09	106.58	106.64
C/F/S-3	117.24	117.29	151.56	151.65	154.14	154.47
C/F/S-4	162.30	161.83	151.91	151.41	139.10	138.69
C/F/S-5	117.24	117.28	118.05	117.70	154.14	154.47
C/F/S-6	130.50	130.45	123.28	123.18	106.58	106.64
C/F/S-7	145.10	145.07	145.29	145.30	145.24	145.31
C/F/S-8	115.90	115.90	116.62	116.51	118.23	118.15
C/F/S-9	167.80	167.78	167.75	167.74	167.55	167.56

[a] See Table II and text for experimental details.

Table IV. ^{13}C NMR Data for the Lignin–Hydroxycinnamyl Ether-Linked Model Dimer Peracetates[a]

	12b		13b		14b	
carbon	*threo*	*erythro*	*threo*	*erythro*	*threo*	*erythro*
α	75.02	74.12	75.22	74.38	76.33	74.99
β	78.86	78.54	80.33	79.87	81.74	81.57
γ	63.23	62.88	63.47	62.95	64.20	63.26
A-1	136.28	136.39	136.44	136.40	137.07	136.97
A-2	112.63	112.66	112.65	112.81	112.63	112.21
A-3	152.33	152.16	152.24	152.10	152.11	152.09
A-4	141.05	140.88	140.96	140.84	140.80	140.61
A-5	120.42	120.35	123.59	123.35	123.46	123.34
A-6	123.71	123.51	120.33	120.48	120.27	119.96
C/F/S-1	128.88	128.96	129.98	130.19	130.89	131.17
C/F/S-2	130.69	130.68	112.37	112.45	106.35	106.32
C/F/S-3	117.32	117.47	151.71	151.89	154.05	154.29
C/F/S-4	161.40	160.86	151.08	150.32	139.65	138.40
C/F/S-5	117.32	117.47	118.03	118.48	154.05	154.29
C/F/S-6	130.69	130.68	122.99	122.91	106.35	106.32
C/F/S-7	144.78	144.75	145.12	145.08	145.45	145.42
C/F/S-8	116.67	116.72	117.07	117.16	117.92	118.04
C/F/S-9	167.66	167.64	167.66	167.64	167.58	167.57

[a] See Table II and text for experimental details.

B. Carbon Assignments. The ^{13}C NMR data for the final products are shown in Tables II–IV. Chemical shifts are to within ±0.01 ppm. As described under Experimental Methods, efforts were made to analyze 15–25 mg of each sample in acetone-d_6 at 27 °C. This was sufficient sample for an excellent spectrum to be obtained with less than 1024 scans (<45 min). It was observed that insufficient temperature control (i.e., ambient temperature) resulted in chemical shift differences on the order of 0.02–0.14 ppm. These differences became important, especially when the chemical shifts of the threo and erythro isomers were compared. Samples were not exchanged with D_2O prior to acquisition of the ^{13}C spectra as this led to significant reduction in the intensity of the carbon signals of the positions that possessed hydroxyl functionality.

The carbon chemical shift assignments shown in Tables II–IV were determined from analysis of COSY and TOCSY ^1H–^1H homonuclear experiments in concert with the results of inverse-detected one-bond (HMQC; Bax and Subramanian, 1986) and long-range (HMBC; Bax and Summers, 1986) ^1H–^{13}C correlation experiments. The general method of assigning the carbons is outlined for 5-*erythro*. The routine acquistion of ^{13}C, DEPT (DEPT135; CH_2's down, CH_3's and CH's up, quaternary carbons not observed), and ^1H spectra provides the necessary information to perform an HMQC experiment with the appropriate sweep widths. Acquisitions using 8 scans of 256 increments (2K data points, 1-h run time) were sufficient or excessive for all samples, including the α-etherified trimers, as can be seen in Figure 2, where the

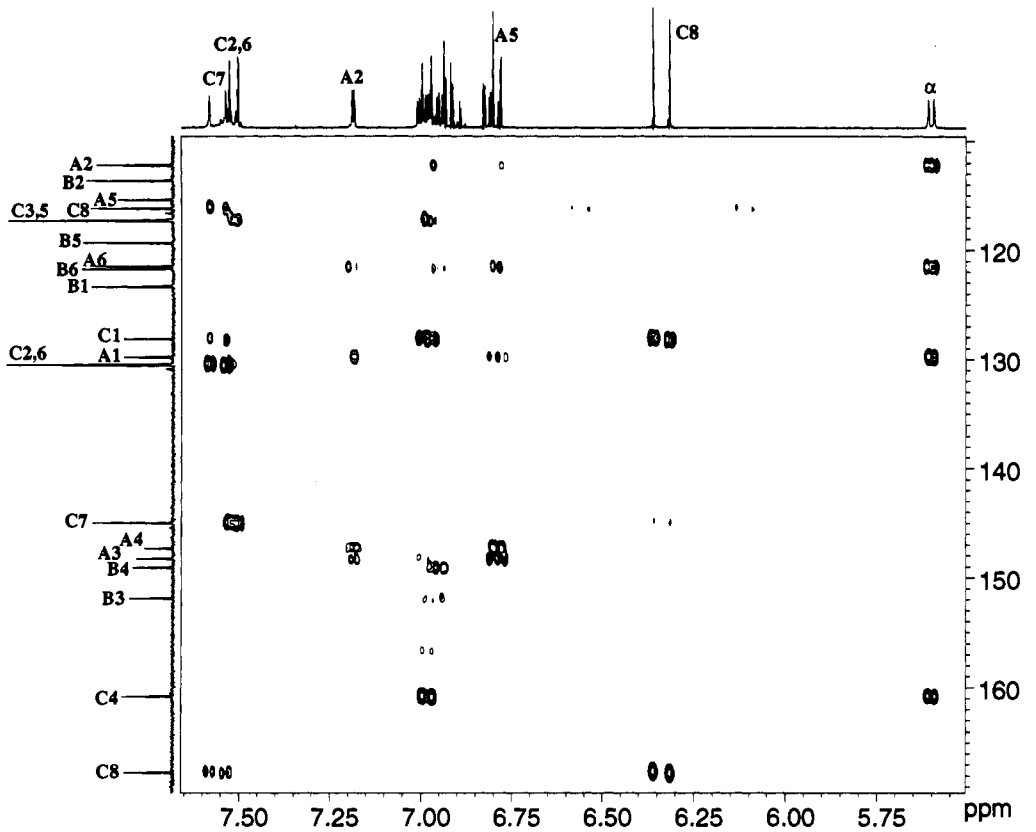

Figure 3. Portion of the HMBC spectrum of 5-*erythro* in which correlations of protons and carbons which are three bonds apart are maximized.

congested aromatic region of the one-bond (HMQC) experiment is shown. The downfield doublet at 7.18 ppm has a small meta coupling and is therefore the A-2 proton. Its meta-coupling partner, A-6 (dd), has an ortho-coupling, A-5 (d), which are all readily observed in COSY and TOCSY spectra. This information allows the assignment of the A-2, A-6, and A-5 carbons.

The C-ring side-chain carbons, C-7 (144.96 ppm) and C-8 (116.19), are assigned on the basis of their correlation to protons which possess large coupling constants ($J = 16$ Hz), while C-9 (167.71 ppm) is readily assigned as the only carbonyl carbon in the molecule. The assignments of C-3,5 (117.21) and C-2,6 (130.44) are based on the established chemical shifts of *p*-coumaryl derivatives (Himmelsbach and Barton, 1980; Helm et al., 1992).

The B-ring methine carbons are the most difficult to assign, and very little information can be obtained from the one-bond correlation experiment. Complete assignment of the B-ring carbons as well as the quaternary carbons can be accomplished with the aid of the long-range HMBC experiment. This two-dimensional experiment maximizes correlations between protons and carbons which are three bonds apart, although occasionally two-bond correlations are also evident. A portion of the 2D spectrum for 5-*erythro* is shown in Figure 3.

The α-proton has strong correlations to carbons A-2, A-1, A-6, and C-4. It has been our observation that the ability of the α-proton to correlate with so many neighboring carbons makes the HMBC experiment a distinct improvement over the carbon-detected long-range experiment. The A- and B-ring methoxyls have very intense correlations with their respective A-3 and B-3 carbons (not shown), which allows for their unambiguous assignment. Having assigned carbons A-3 and B-3, the remaining two carbons in that region of the spectrum are carbons A-4 and B-4. The correlation of the peak at 147.31 with the A-2 and A-6 protons implies that this carbon is A-4 and the remaining carbon at 149.85 is B-4. The correlation between the C-1 carbon and the C-8 and C-3,5 protons confirms all C-ring assignments. The B-4 carbon correlates with the β-proton as well as the B-2 and B-6 protons. These correlations are at times very weak, and processing the serial files with different sine-bell-squared apodization functions (Q0 or Q2) helps to maximize the correlations of interest. The designation of the multiplet at 6.81 ppm (^{1}H spectrum) as proton B-6 implies that the multiplet at 6.81 ppm is the B-1 proton. The B-ring assignments match those of Ralph (1988) for 1-*erythro*, where the carbon-detected long-range technique was employed. Thus, the assignment of 5-*erythro* is complete, and in this manner unambiguous assignments for the other models were determined.

The ^{13}C chemical shifts of the threo/erythro models are very similar, as can be seen by reviewing Tables II–IV. The major differences are with the carbons closest to the site of stereochemical difference. The erythro α, B-4, and C/F-4 carbons of the α-ether trimers are of lower chemical shifts than their corresponding threo counterparts (Table II). The same trend also holds for the appropriate β-*O*-4 cinnamyl dimer carbons (Table III) and their peracetates (Table IV). The chemical shifts of the β-carbons of the β-cinnamyl models (Table III) increase as one proceeds from *p*-coumaryl, to feruyl, to sinapyl substituent. This effect is somewhat moderated by acetylation (Table IV).

Summary. Ether-linked models that represent the major theorized lignin–hydroxycinnamyl ether condensation products have been prepared and characterized by NMR spectroscopy. The β-cinnamyl ethers, used for modeling products active in copolymerization of cinnamyl groups and lignin monomers, were prepared by modifying an established route to β-*O*-4 models. The use of two different reducing agents afforded both threo and erythro

isomers. The α-cinnamyl ethers, which represent passive or opportunistic incorporation of hydroxycinnamyl groups into lignin, were prepared by a base-catalyzed addition of the phenolate anion to **1a**. The overall yields and isomeric ratios were dependent on both the phenol and the total reaction time. The instability of 6-*erythro* in aqueous environments suggests that its presence in native lignins may be insignificant. Spectroscopic characterization provides important chemical shift information for the growing NMR database related to lignin structure and will prove to be invaluable in future studies related to the structure and function of forage lignins.

ACKNOWLEDGMENT

This work was supported in part by a grant from the USDA Competitive Grants Program (Plant Growth and Development, 90-37261-5617). We thank the Department of Chemistry, University of Wisconsin—Madison, for use of their NMR facilities during the initial stages of these investigations, as well as the USDA Agricultural Research Service and the U.S. Dairy Forage Research Center for funding the purchase of the Bruker AMX-360 spectrometer, which was used throughout the latter stages of this work.

LITERATURE CITED

Allen, P. J. Specificity of the *cis*-Isomers of Inhibitors of Uredospore Germination in the Rust Fungi. *Proc. Natl. Acad. Sci. U.S.A.* **1972**, *69*, 3497–3500.

Bacic, A.; Harris, P. J.; Stone, B. A. Structure and Function of Plant Cell Walls. In *Biochemistry of Plants*; Preiss, J., Ed.; Academic Press: New York, 1988; Vol. 14, Chapter 8.

Barrelle, M.; Béguin, C. G.; Tetaz, F. NMR Conformational Investigation of Stereocontrolled Reduction of Lignin-Model Compounds. *Holzforschung* **1989**, *43*, 339–343.

Bax, A.; Davis, D. G. MLEV-17-Based Two-Dimensional Homonuclear Magnetization Transfer Spectroscopy. *J. Magn. Reson.* **1985**, *65*, 355–360.

Bax, A.; Subramanian, S. Sensitivity-Enhanced Two-Dimensional Heteronuclear Shift Correlation NMR Spectroscopy. *J. Magn. Reson.* **1986**, *67*, 565–569.

Bax, A.; Summers, M. F. ^{1}H and ^{13}C Assignments from Sensitivity-Enhanced Detection of Heteronuclear Multiple-Bond Connectivity by 2D Multiple Quantum NMR. *J. Am. Chem. Soc.* **1986**, *108*, 2093–2094.

Brunow, G.; Sipilä, J.; Lundquist, K.; Unge, S. V. The Preparation of *Threo* Forms of β-O-4 Lignin Model Compounds. *Cell. Chem. Technol.* **1988**, *22*, 191–199.

Brunow, G.; Sipilä, J.; Mäkelä, T. On the Mechanism of Formation of Non-cyclic Benzyl Ethers During Lignin Biosynthesis. *Holzforschung* **1989**, *43*, 55–59.

Ede, R. M.; Brunow, G. Application of Two-Dimensional Homo- and Heteronuclear Correlation NMR Spectroscopy to Wood Lignin Structure Determination. *J. Org. Chem.* **1992**, *57*, 1477–1480.

Ede, R.; Main, L.; Ralph, J. Evidence for Increased Steric Compression in *Anti* Compared to *Syn* Lignin Model Quinone Methides. *J. Wood Chem. Technol.* **1990**, *10*, 101–110.

Freudenberg, K.; Friedmann, M. *Chem. Ber.* **1960**, *93*, 2138–2148.

Fry, S. C.; Miller, J. K. Toward a Working Model of the Growing Plant Cell Wall: Phenolic Cross-Linking Reactions in the Primary Cell Walls of Dicotyledons. In *Plant Cell Wall Polymers: Biogenesis and Degradation*. Lewis, N. G., Paice, M. G., Eds.; ACS Symposium Series 299; American Chemical Society: Washington, DC, 1989; pp 33–46.

Gensler, W. J.; Johnson, F.; Sloan, A. D. B. Compounds Related to Podophyllotoxin. XII. Podophyllotoxone, Picrophyllonone, and Dehydropodopyllotoxin. *J. Am. Chem. Soc.* **1960**, *82*, 6074–6081.

Greene, T. W.; Wuts, P. G. M. In *Protective Groups in Organic Synthesis*, 2nd ed.; Wiley-Interscience: New York, 1991; pp 162–163.

Helm, R. F.; Ralph, J.; Anderson, L. Regioselective Protective Strategies for D-Xylopyranosides. *J. Org. Chem.* **1991**, *56*, 7015–7021.

Helm, R. F.; Ralph, J.; Hatfield, R. D. Synthesis of *p*-Coumaroylated and Feruloylated Methyl Glycosides. *Carbohydr. Res.* **1992**, *229*, 183–194.

Himmelsbach, D. S.; Barton, F. E. ^{13}C Nuclear Magnetic Resonance of Grass Lignins. *J. Agric. Food Chem.* **1980**, *28*, 1202–1208.

Iiyama, K.; Lam, T. B. T.; Stone, B. A. Phenolic Acid Bridges Between Polysaccharides and Lignin in Wheat Internodes. *Phytochemistry* **1990**, *29*, 733–737.

Ishii, T. Isolation and Characterization of a Diferuloyl Arabinoxylan Hexasaccharide From Bamboo Shoot Cell-Walls. *Carbohydr. Res.* **1991**, *219*, 15–22.

Katayama, T.; Nakatsubo, F.; Higuchi, T. Synthesis of Arylglycerol-β-Aryl Ethers. *Mokuzai Gakkaishi* **1981**, *27*, 223–230.

Katayama, T.; Kawai, S.; Sogo, M.; Higuchi, T. Degradation of Guaiacylglycerol-α-Vanillyl Alcohol-β-Vanillin Diether, a Lignin Substructure Model Containing a Non-Cyclic Benzyl Aryl Ether, by *Fusarium solani* M-13-1. *Mokuzai Gakkaishi* **1987**, *33*, 503–510.

Kondo, T.; Mizuno, K.; Kato, T. Cell Wall-Bound *p*-Coumaric and Ferulic Acids in Italian Ryegrass. *Can. J. Plant Sci.* **1990**, *71*, 495–499.

Lam, T. B. T.; Iiyama, K.; Stone, B. A. Distribution of Free and Combined Phenolic Acids in Wheat Internodes. *Phytochemistry* **1990**, *29*, 429–433.

Lam, T. B. T.; Iiyama, K.; Stone, B. A. Cinnamic Acid Bridges Between Cell Wall Polymers in Wheat and Phalaris Internodes. *Phytochemistry* **1992**, *31*, 1179–1183.

Landucci, L. L.; Geddes, S. A.; Kirk, T. K. Synthesis of ^{14}C Labeled 3-Methoxy-4-Hydroxy-α-(2-Methoxy-phenoxy)-β-Hydroxypropiophenone, a Lignin Model Compound. *Holzforschung* **1981**, *35*, 66–69.

Leary, G.; Miller, I. J.; Thomas, W.; Woolhouse, A. D. The Chemistry of Reactive Lignin Intermediates. Part 5. Rates of Reactions of Quinone Methides with Water, Alcohols, and Carboxylic Acids. *J. Chem. Soc., Perkin Trans. 2* **1977**, *13*, 1737–1739.

Lewis, N. G.; Yamamoto, E. Lignin: Occurrence, Biogenesis and Biodegradation. *Annu. Rev. Plant Physiol. Plant Mol. Biol.* **1990**, *41*, 455–496.

Mueller-Harvey, I.; Hartley, R. D.; Harris, P. J.; Curzon, E. H. Linkage of *p*-Coumaroyl and Feruloyl Groups to Cell-Wall Polysaccharides of Barley Straw. *Carbohydr. Res.* **1986**, *148*, 71–85.

Nakata, T.; Oishi, T. Stereoselective Reduction of β-keto Esters with Zinc Borohydride. Stereoselective Synthesis of *Erythro*-3-hydroxy-2-alkylpropionates. *Tetrahedron Lett.* **1980**, *21*, 1641–1644.

Nakatsubo, F.; Sato, K.; Higuchi, T. Synthesis of Guaiacylglycerol-β-guaiacyl Ether. *Holzforschung* **1975**, *29*, 165–168.

Nakatsubo, F.; Sato, K.; Higuchi, T. Enzymic Dehydrogenation of *p*-Coumaryl Alcohol. IV. Reactivity of Quinonemethide. *Mokuzai Gakkaishi* **1976**, *22*, 29–33.

Ralph, J. NMR of Lignin Model Compounds; Application of Long-range C-H Correlations Through Oxygen. *Holzforschung* **1988**, *42*, 273–275.

Ralph, J.; Helm, R. F. Rapid Proton NMR Method for Determination of *Threo*:*Erythro* Ratios in Lignin Model Compounds and Examination of Reduction Stereochemistry. *J. Agric. Food Chem.* **1991**, *39*, 705–709.

Ralph, J.; Helm, R. F. The Lignin-Hydroxycinnamic Acid-Polysaccharide Complex: Synthetic Models for Regiochemical Characterization. In *Forage Cell Wall Structure and Digestibility*; Jung, H.-J. G., Buxton, D. R., Hatfield, R. D., Ralph, J., Eds.; American Society of Agronomy: Madison, WI, 1992, in press.

Ralph, J.; Young, R. A. Synthesis of the Lignin Model Compounds *Threo*-Guaiacylglycerol-β-Guaiacyl Ether and *Threo*-Veratrylglycerol-β-Guaiacyl Ether. *Holzforschung* **1981**, *35*, 39–41.

Ralph, J.; Young, R. A. Stereochemical Aspects of Addition Reactions Involving Lignin Model Quinone Methides. *J. Wood Chem. Technol.* **1983**, *3*, 161–181.

Ralph, J.; Elder, T. J.; Ede, R. M. The Stereochemistry of Guaiacyl Lignin Model Quinone Methides. *Holzforschung* **1991**, *45*, 199–204.

Ralph, J.; Helm, R. F.; Quideau, S.; Hatfield, R. D. Lignin-Feruloyl Ester Cross-Links in Grasses. 1. Incorporation of Feruloyl Esters into Coniferyl Alcohol Dehydrogenation Polymers. *J. Chem. Soc., Perkin Trans. 1* **1992a**, in press.

Ralph, J.; Helm, R. F.; Quideau, S. Lignin-Feruloyl Ester Cross-Links in Grasses. 2. Model Compound Syntheses. *J. Chem. Soc., Perkin Trans. 1* **1992b**, in press.

Scalbert, A.; Monties, B.; Lallemand, J.-Y.; Guittet, E.; Rolando, C. Ether Linkage Between Phenolic Acids and Lignin Fractions from Wheat Straw. *Phytochemistry* **1985**, *24*, 1359–1362.

Scalbert, A.; Monties, B.; Rolando, C.; Sierra-Escudero, A. Formation of Ether Linkage Between Phenolic Acid and Gramineae Lignin: A Possible Mechanism Involving Quinone Methides. *Holzforschung* **1986**, *40*, 191–195.

Yamamoto, E.; Bokelman, G. H.; Lewis, N. G. Phenylpropanoid Metabolism in Cell Walls. An Overview. In *Plant Cell Wall Polymers: Biogenesis and Degradation*; Lewis, N. G., Paice, M. G., Eds.; ACS Symposium Series 299; American Chemical Society: Washington, DC, 1989; pp 68–88.

Received for review June 3, 1992. Accepted July 20, 1992. Mention of a trade name, proprietary product, or specific equipment does not constitute a guarantee of the product by the USDA and does not imply its approval to the exclusion of other products that might also be suitable.

Registry No. *threo*-**1**, 143614-36-2; *erythro*-**1**, 143563-69-3; **1a**, 143563-70-6; **2**, 3943-97-3; **3**, 2309-07-1; **4**, 20733-94-2; *erythro*-**5**, 143494-34-2; *threo*-**5**, 143494-33-1; *threo*-**5a**, 143494-54-6; *erythro*-**5a**, 143494-53-5; *threo*-**6**, 143507-89-5; *erythro*-**6**, 143494-35-3; *threo*-**6a**, 143494-55-7; *erythro*-**6a**, 143494-56-8; **7**, 498-02-2; **8**, 50893-83-9; **9**, 143494-36-4; **9a**, 143494-39-7; **10**, 143494-37-5; **10a**, 143507-90-8; **11**, 143494-38-6; **11a**, 143507-91-9; *threo*-**12**, 143494-41-1; *erythro*-**12**, 143494-40-0; *threo*-**12a**, 143494-46-6; *erythro*-**12a**, 143494-45-5; *threo*-**12b**, 143494-49-9; *erythro*-**12b**, 143507-74-8; *threo*-**13**, 143494-43-3; *erythro*-**13**, 143494-42-2; *threo*-**13a**, 143494-48-8; *erythro*-**13a**, 143494-47-7; *threo*-**13b**, 143507-75-9; *erythro*-**13b**, 143494-50-2; *threo*-**14**, 143494-44-4; *erythro*-**14**, 143507-73-7; *threo*-**14a**, 143563-72-8; *erythro*-**14a**, 143563-71-7; *threo*-**14b**, 143494-52-4; *erythro*-**14b**, 143494-51-3; *p*-coumaric acid, 7400-08-0; 3,5-dimethoxy-4-hydroxy-*trans*-cinnamic acid, 7362-37-0; 4-acetoxy-3-methoxyacetophenone, 54771-60-7.